SMALL ANGLE ELASTIC SCATTERING OF 660 MeV PROTONS ON CARBON NUCLEI

L. S. AZHGIREĬ, Yu. P. KUMEKIN, M. G. MESHCHERYAKOV, S. B. NURUSHEV, G. D. STOLETOV and HUANG TIEH-CH'IANG

Joint Institute for Nuclear Research

Submitted to JETP editor June 30, 1963

J. Exptl. Theoret. Phys. (U.S.S.R.) 44, 177—191 (January, 1963)

The differential cross section for elastic scattering of 660-MeV protons by carbon nuclei and the polarization arising as a result of the scattering are measured in the range $1.8° \leq \theta \leq 9°$. Elastic proton scattering was separated from the inelastic processes by the magnetic analysis method. The following best values for the real and imaginary parts of the spin-independent and spin-dependent amplitudes were derived from the experimental data: $g_{NR}(0) = -5.05 \pm 0.45$, $g_{NI}(0) = 15.26 \pm 0.45$; $h_{NR}(0) = -10.4 \pm 13.3$, and $h_{NI}(0) = 37.6 \pm 9.3$ (in 10^{-13} cm units). The potentials of the integrated optical model are estimated. The root mean square radii for the central and spin-orbit potentials are found to be $(2.48 \pm 0.04) \times 10^{-13}$ and $(2.83 \pm 0.16) \times 10^{-13}$ cm, respectively. It is demonstrated that the spin-orbit interaction decreases with the energy. It is concluded that at 660 MeV the spin-orbit potential for nucleon-nucleus interaction is complex.

1. INTRODUCTION

ELASTIC scattering of high-energy protons ($E \geq 100$ MeV) by complex nuclei has been the object of numerous experimental and theoretical investigations [1]. With respect to experiment, this problem is made complicated by the difficulties connected with the separation of the protons that have experienced only elastic (diffraction) scattering from the inelastically scattered particles. The simplest theoretical analysis of elastic scattering of nucleons by complex nuclei in the angle interval below the first diffraction minimum is based on the use of the semiclassical approximation [2-5].

The matrix of elastic scattering of a nucleon by a spinless pointlike nucleus has the form [6]

$$f_N(q) = g_N(q) + h_N(q)\,\sigma_n, \qquad (1)$$

where $G_N(q) = G_{NR} + ig_{NI}$ and $h_N(q) = h_{NR} + ih_{NI}$ are functions of the energy and of the scattering angle θ; $q = 2k \sin(\theta/2)$; k is the magnitude of the wave vector of the nucleon in the laboratory system; σ_n is the projection of the spin operator on the normal to the scattering plane. In the region of small angles, the amplitude $h_N(q)$, which depends on the nucleon spin, can be represented in the form

$$h_N(q) = h_N(0) \sin\theta. \qquad (2)$$

To determine the amplitude $g_N(q)$ and $H_N(q)$ with accuracy to a common phase factor, it is necessary to carry out a complete experiment which includes measurement of the differential cross section $d\sigma/d\omega(\theta)$ for the elastic scattering of the protons from an unpolarized beam, their polarization $P(\theta)$, and one of the triple-scattering parameters (R or A). Observation of interference between the nuclear and Coulomb scatterings in the small-angle region yields additional information on the amplitudes $g_N(q)$ and $h_N(q)$.

In the present article we describe experiments in which the differential cross sections $d\sigma/d\omega(\theta)$ for the elastic scattering of 660-MeV protons by carbon nuclei and the polarization of these protons $P(\theta)$ were measured in order to obtain the data necessary for the determination of the forward-scattering amplitudes $g_{NR}(0)$, $g_{NI}(0)$, $h_{NR}(0)$, and $h_{NI}(0)$, and the corresponding nuclear potentials of the optical model. The measurements were carried out in the small-angle interval in which the interference between the nuclear and Coulomb scatterings manifests itself. The procedure developed in these experiments made it possible to exclude to a considereable degree the influence of the accompanying inelastic processes.

The experiments were made with the six-meter synchrocyclotron of the Joint Institute for Nuclear Research.

[1] A complete summary of the published experimental and theoretical papers is contained, for example, in the review by Faissner [1].

2. EXPERIMENT

A. Measurement of the secondary-particle energy spectra. The energy spectra of the secondary particles due to pC collisions were measured in order to separate the diffraction scattering of the protons by the carbon nuclei from the accompanying inelastic processes at the angles 4.2, 5.2, 7.0, 8.3, 9.1, and 10.7°. The direction of the primary beam and the location of the scatterer T_1 in it (see Fig. 1a) were chosen such that the secondary-particle beam, scattered through the specified angle θ_1 and separated by the collimators K_1 and K_2, was aimed at the center of the magnet. The proton energy at the location of the scatterer T_1 was 660 ± 3.0 MeV. The secondary particles, after passing through the analyzing field and the collimators K_3 in a four-meter shielding wall, were registered either by a telescope of three scintillation counters or by the argon-filled ionization chamber M_2. The relative width $\Delta p/p$ of the momentum interval separated by the analyzer was ~ 1.7% over the entire extent of the investigated spectra. From the number of secondary particles at the output of the analyzer, measured as a function of the magnetic field intensity, we plotted the relative momentum spectrum at equal $H\rho$ intervals. The spectrum was then transformed into an energy spectrum under the assumption that the secondary particles were protons.

The curves on Fig. 2 are typical secondary-proton energy spectra near the diffraction peaks. It is seen how the characteristic "congestion" corresponding to the protons that have lost part of their energy to excitation of the carbon nuclei becomes more and more noticeable with increasing angle of observation in each spectrum on the left side of the diffraction peak. The possibility of attributing these ledges to the partial slowing down of the protons as they pass through the collimating unit of the analyzer is excluded, since the peaks corresponding to protons from elastic pp scattering, observed in exactly the same manner and under the same angles, had a strictly symmetrical form.

The diffraction-scattered protons were separated from the remaining secondary particles by subtraction of the areas under the curves which represented, on the one hand, the energy spectrum of the protons

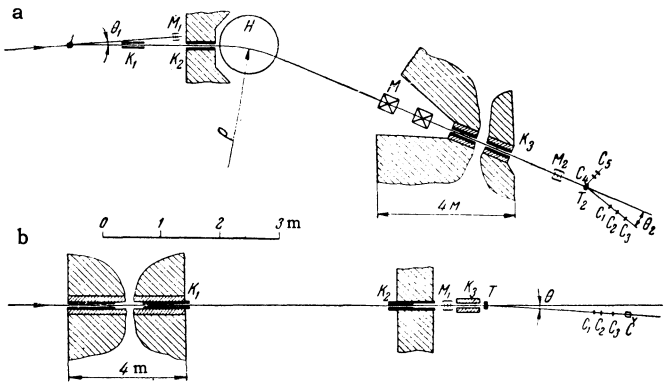

FIG. 1. Diagram of experimental setups: a – for measurement of the polarization of protons elastically scattered by carbon nuclei (T_1 – polarizer, T_2 – polarization analyzer, H – analyzing magnet, K_1, K_2, K_3 – collimators, M_1 and M_2 – monitors, M – quadrupole lenses, C_1 to C_5 – scintillation counters); b – for the measurement of the differential cross sections of scattering by carbon (K_1, K_2, K_3 – collimators, M_1 – monitor, T – carbon scatterer, C_1, C_2, C_3 – scintillation counters, Č – Cerenkov counter).

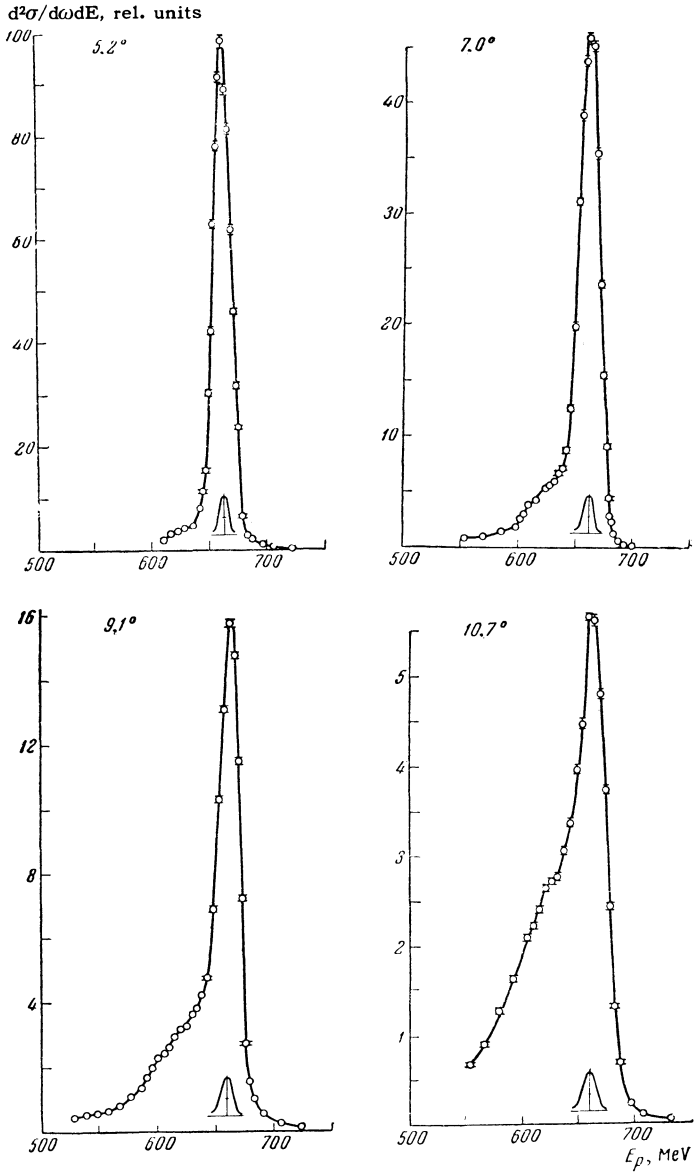

FIG. 2. Typical energy spectra of protons emitted at different angles θ in pC collisions at 660 MeV. Under the diffraction peaks are shown the instrumental resolution of the measurement of the proton polarization.

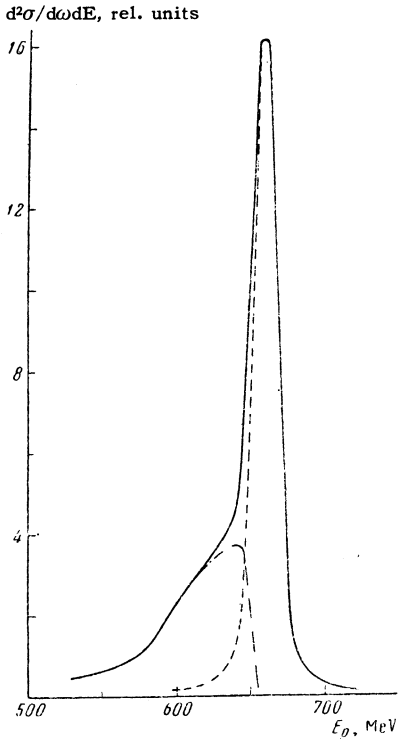

FIG. 3. Separation of the pC inelastic-scattering spectrum for $\theta = 9.1°$. Continuous curve – summary spectrum of secondary protons from pC collisions; short dashes – left side of the peak, corresponding to protons from the elastic pp scattering (this peak is shifted to the right by an amount equal to the difference in the proton energies in elastic pC and pp scattering); long dashes – difference curve, representing the spectrum of the protons that have experienced slightly inelastic scattering.

from the pC collisions, and on the other the peak corresponding to the protons from the elastic pp scattering in a polyethylene scatterer. The diffraction peak from the pC collisions and the peak from the elastic pp scattering were normalized to equal height and their maxima were aligned. Since the energy spread of the primary beam and the resolution of the analyzer remained the same when the graphite scatterer was replaced by polyethylene, it was to be expected that the form of these peaks and their width at half height would be the same. This was confirmed by the fact that when the peaks were aligned their right-hand branches always coincided. By way of an example, Fig. 3 shows for $\theta = 9.1°$ the result of the subtraction of the areas under the normalized peaks, and the thus-separated diffraction peak and the spectrum of the protons that have experienced slightly inelastic scattering.

An analysis of the spectra has shown that slightly inelastic scattering of protons competes noticeably with elastic scattering on C^{12} nuclei even in the region of angles much below the first diffraction minimum, and that the energy most frequently transferred to the nucleus does not depend on the angle and corresponds approximately to the position of the maximum of the giant photoresonance of C^{12}. However, the spectrum of the slightly inelastically scattered protons was considerably broader than the region of the giant photoresonance of C^{12} at all angles of observation, something that cannot be attributed to either the energy spread of the primary beam or to the finite resolution of the analyzer. In this connection, it is quite likely that inelastic small-angle scattering of fast protons leads frequently to the occurrence in nuclei of spin-wave excitations that do not manifest themselves in ordinary photonuclear transitions [7,8].

These results offer evidence that even at relatively high energies (E > 600 MeV) reliable information on the differential cross section for small-angle elastic scattering of protons by nuclei and the polarization of the protons in this process can be obtained only when the elastically scattered protons are carefully separated from the protons that have experienced slightly inelastic scattering.

B. Determination of the differential cross section of pC scattering. The experimental setup is shown in Fig. 1b. The unpolarized proton beam is deflected 14.2° on its path to collimators K_1—K_3 by the auxillary magnetic field. The neutral and low-energy particles are at the same time removed from the beam. The geometrical collimation was such that the following happened at the location of the scatterer: a) the beam image had a height of 20 mm and a width of 10 mm; b) the beam divergence in the horizontal plane was ± 0.15°. All measures were taken to reduce to a minimum the scattering of protons in the collimator walls.

The scattered protons were registered with a telescope made up of three scintillation counters C_1, C_2, and C_3, and one Cerenkov counter $\check{C}$ with Plexiglas radiator. The angular resolution was determined essentially by the multiple scattering of the protons in the scatterer and amounted to ± 0.3°. In order to reduce the error in the adjustment of the apparatus and to prevent the drift from affecting the radio circuitry, the usual procedure was followed, of making frequently alternating measurements of the angular distributions of the scattered protons to the right and to the left of the primary beam with subsequent introduction of the correction (~ 0.05°) to the readings on the angle scale. Simultaneously, we registered the counting rates N_{123} of the triple coincidences of pulses from the scintillation counters, corresponding to the same solid angle 2×10^{-4} sr (the threshold energy of the registered protons was 60 MeV in this case), and the number

of coincidences $N_{123\check{C}}$ of the pulses from all four counters.

The diffraction scattering of the protons and the absolute values of the differential cross sections of this process were determined in the following manner. The averaged measured counting rates N_{123} to the right and to the left of the beam were used to plot an angular distribution curve for the secondary charged particles, and this curve was then normalized in the overlapping observation-angle zone to the absolute values of the differential cross sections for the emission of secondary charged particles in pC collisions, obtained previously [9] under conditions identical with those of the present experiment. The total energy spectrum of secondary charged particles measured at 7° was also normalized to the differential cross section obtained for this angle in [9] namely $(1.100 \pm 0.055) \times 10^{-24}$ cm^2/sr.

A comparison of the readings of the $(C_1C_2C_3)$ and $(C_1C_2C_3\check{C})$ telescopes has shown that in the range of angles under consideration the values of N_{123} and $N_{123\check{C}}$ are connected by the relation $N_{123\check{C}} = (0.452 \pm 0.005)(N_{123} - Q)$, where Q is a constant. Apart from a factor that takes into account the efficiency of the Cerenkov counter, Q represents the difference between the number of protons registered by the $(C_1C_2C_3)$ telescope, on the one hand, and by the $(C_1C_2C_3\check{C})$ telescope on the other, i.e., the number of protons that have experienced elastic interaction with large energy loss. This relation between N_{123} and $N_{123\check{C}}$ can be interpreted as if the detecting system discerned in the spectra two groups of protons: one, numbering $N_{123} - Q$ and located above a certain energy threshold E_C, is registered by a Cerenkov counter with average efficiency $\epsilon = 0.452 \pm 0.005$, while the other, numbering Q and located below the energy E_C, is not registered by the Cerenkov counter at all.

A comparison of the values of N_{123} and Q has shown that the number of protons Q corresponds to a differential cross section $(207 \pm 19) \times 10^{27}$ cm^2/sr. Corresponding to this cross section and to the spectrum measured at 7° is an interval extending up to $E_{\check{C}} = 610$ MeV. Since the value of Q remained unchanged in the considered range of angles, it can be stated that in the present experiments the protons not registered by the Cerenkov counter were distributed approximately isotropically and that the threshold energy $E_{\check{C}}$ lies in approximately the same region of the spectra. Indeed, an analysis of the spectrum measured at 12.2° has shown that the low-energy part of the spectrum, which makes a contribution equal to $(207 \pm 19) \times 10^{-27}$ cm^2/sr extends from 60 to 608 MeV.

The energy spectra at 4.1, 5.2, 8.3, 9.1, and 10.7° were measured only above 610 MeV (some of the spectra are shown in Fig. 2).

In all cases, the spectra of the slightly elastically scattered protons were separated from the diffraction peaks as described in item A of Sec 2. The differential cross sections obtained for the indicated angles and corresponding to the energy interval from 610 MeV up to the upper limit of the spectrum of the slightly inelastically scattered protons can be approximated by a straight line, extrapolation of which in the angle region $1.8° \leq \theta < 4.1°$ has enabled us to estimate the contribution of the energy interval under consideration to the total yield of the secondary particles. According to the estimate, the pion admixture among the elastically scattered protons was negligibly small.

Figure 4 shows the values of the differential

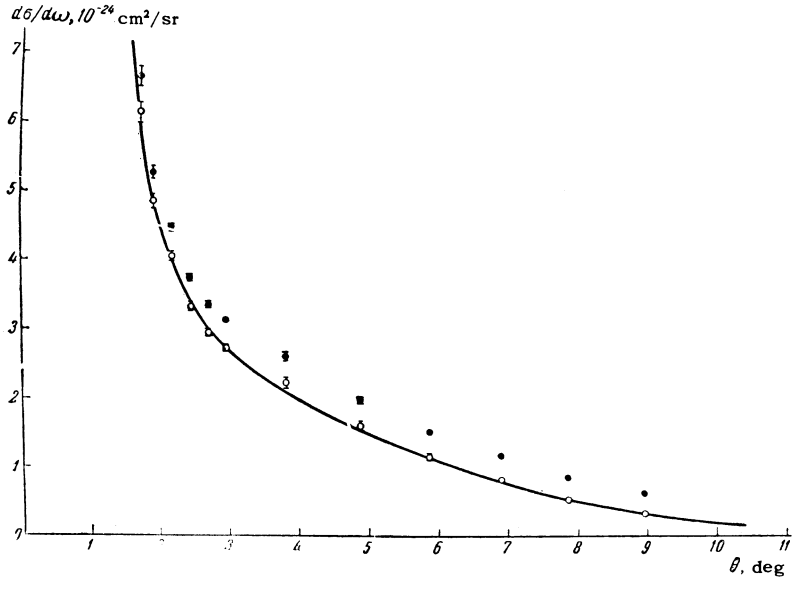

FIG. 4. Differential cross sections for the scattering of protons by carbon nuclei at 660 MeV. The experimental points correspond to: ● – secondary protons with energy above 60 MeV; o – elastically scattered protons. The continuous curve represents the calculated dependence of $d\sigma/d\omega$ on θ (variant IV).

cross sections for the emission of protons with energy from 60 MeV to the upper limit of the spectrum, obtained in this manner, as well as the values of the differential cross section of the elastic (diffraction) scattering of protons together with the statistical measurement errors.

C. Measurement of proton polarization in elastic pC scattering. The experimental procedure consists of first separating with the aid of a magnetic analyzer the diffraction peak from the spectrum of the secondary particles due to the pC collisions in the polarizer T_1, and then measuring the proton polarization in this peak. The analysis was by elastic scattering of the protons by protons in the polyethylene analyzer T_2 (Fig. 1a). The mean proton energy in the separated band corresponded to the maximum of the diffraction peak and was maintained constant during the time of the measurements. As the scattering angle increased from 2.1 to 10.7°, the width of the separated zone at half the altitude increased, in accordance with the estimate, from 8 to 13 MeV. This was accompanied by an increase in the fraction of the admixture of the slightly inelastically scattered protons in the separated band of the spectrum; it did not exceed 3% at 10.7°.

The elastic pp scattering in a polyethylene analyzer 4 mm thick was completely separated from the inelastic processes by means of two conjugated telescopes, (C_1C_2 C_3) and (C_4C_5), installed in accordance with the kinematics of the elastic pp scattering alternately to the right and to the left of the beam passing through the analyzer. The effect due to the carbon was excluded by measuring the difference in the counting rates with the polyethylene and with a graphite analyzer having an equivalent number of carbon nuclei. Standard electronic coincidence circuits were used for the pulses from the scintillation counters and the telescopes, with a resolution time 1×10^{-8} sec.

The asymmetry $\epsilon(\theta_1)$ in the analyzing scattering of the protons previously scattered through an angle θ_1 in the graphite polarizer was measured at $\theta_2 = 18°$. This pp-scattering angle corresponds at 635 MeV, according to Meshcheryakov et al [10] (who measured the polarization in elastic pp scattering by a similar method), to a maximum polarization $P_{pp}(18°) = 0.42 \pm 0.03$. As already noted [10], the magnitude of the polarization and its angular distribution in pp scattering are constant in the energy interval from 415 to 635 MeV. Therefore, assuming that $P_{pp}(18°)$ does not change as the energy increases from 635 to 665 MeV, we could determine the polarization $P_{pC}(\theta_1)$ of the protons in the pC scattering from the relation

$$\varepsilon(\theta_1) = (0{,}42 \pm 0{,}03)\, P_{pC}(\theta_1). \qquad (3)$$

The values of $P_{pC}(\theta_1)$ obtained in this manner in the interval $2.1° \leq \theta_1 \leq 10.7°$ are shown in Fig. 5. We see that the polarization reaches a maximum at $\sim 8.5°$. The possibility of the inelastic processes distorting the observed angular dependence of the polarization has been reduced to a minimum, since only elastic processes have been selected in both the first and the second scattering.

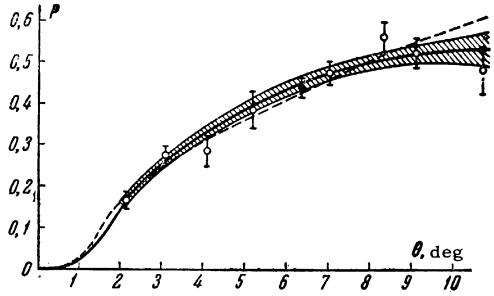

FIG. 5. Polarization of protons symmetrically scattered by carbon nuclei at 660 MeV. The value of P (6.3°) is taken from[11]. The calculated curves correspond to: dashed curve – variant I, solid curve – IV. The shaded strip is the error corridor.

3. CALCULATION OF pC-SCATTERING AMPLITUDES

A. Parametrization of the expressions. The method used in the present work to calculate the amplitudes of the forward pC scattering from the results of small-angle measurements of the differential cross sections of this process and the polarization of scattered protons was developed by Bethe [4] and Cromer [12]. This method is based on the fact that the polarization of the nucleons in nuclear scattering below the first diffraction minimum can be calculated with good accuracy in the Born approximation [2,3]. In this approximation the amplitudes $g_N(q)$ and $h_N(q)$ are proportional to the nuclear form factor

$$F(q) = \frac{4\pi}{q}\int_0^\infty \rho(r)\sin(qr)\, r dr, \qquad (4)$$

where $\rho(r)$ is the distribution of the nucleon density in the nucleus, normalized in such a way that

$$4\pi\int_0^\infty \rho(r)\, r^2 dr = 1.$$

The density of the nucleons is best approximated by a Gaussian distribution

$$\rho(r) = \pi^{-3/2}a^{-3}\exp\{-(r/a)^2\}. \qquad (5)$$

In this case $F(q) = \exp(-a^2q^2/4)$. For the C^{12} nucleus, as follows from experiments on electron scattering [13], the radial parameter of the Gaussian distribution is $a = 1.965 \times 10^{-13}$ cm, which corresponds to a mean square radius $\langle r^2 \rangle^{1/2} = 2.37 \times 10^{-13}$ cm.

The results of the following analysis of the experimental data are to some degree independent of the model employed, since under the conditions of the present experiment ($E = 660$ MeV, $k = 6.56 \times 10^{13}$ cm^{-1}, $1.8° \leq \theta \leq 10.7°$) the values of q lie in the interval $0.21 \leq q \leq 1.22$, in which distribution-density approximations by other than Gaussian functions are in equally good agreement with experiment [13].

Account of the angular dependence of the nucleon-nucleon scattering amplitudes leads to the following expressions for the nucleon-nucleus scattering amplitudes

$$g_{NR}(q) = g_{NR}(0)F_{1R}(q), \quad g_{NI}(q) = g_{NI}(0)F_{1I}(q),$$
$$h_{NR}(q) = h_{NR}(0)\sin\theta \cdot F_{2R}(q),$$
$$h_{NI}(q) = h_{NI}(0)\sin\theta \cdot F_{2I}(q), \qquad (6)$$

where $F_1(q)$ and $F_2(q)$ are the nuclear form factors, which differ from the form factor $F(q)$ obtained in the electron-scattering experiments. Expressions (6) signify that the real and imaginary parts of the central and spin-orbit optical potentials should have a different radial dependence. The available experimental data on the pC scattering at 660 MeV are insufficient to determine, along with the amplitudes $g_{NR}(0)$, $g_{NI}(0)$, $h_{NR}(0)$ and $h_{NI}(0)$, the four other radial parameters of the form factors indicated above with equally good accuracy. We have therefore made the simplifying assumption

$$F_{1R}(q) = F_{1I}(q) = F_1(q) = \exp(-\tfrac{1}{4}a_g^2q^2),$$
$$F_{2R}(q) = F_{2I}(q) = F_2(q) = \exp(-\tfrac{1}{4}a_h^2q^2).$$

The six free parameters (the four amplitudes and the radial parameters a_g and a_h) were varied in such a way as to reconcile them in best manner with the experimental data.

The total proton scattering amplitude is given by the sum of the nuclear and Coulomb scattering amplitudes:

$$g(q) = g_N(q) + g_C(q), \quad h(q) = h_N(q) + h_C(q), \qquad (7)$$

where the Coulomb scattering amplitudes are

$$g_C(q) = -\frac{2nk}{q^2}\left[1 + 2in\ln\left(\frac{\theta_0}{\theta}\right)\right]F(q),$$
$$h_C(q) = -i\sin\theta \cdot \frac{\hbar^2k^2}{2M^2c^2}\left(\mu - \frac{1}{2}\right)g_C(q), \qquad (8)$$

and the nuclear scattering amplitudes are

$$g_N(q) = [g_{NR}(0) + ig_{NI}(0)]\exp\left(-\tfrac{1}{4}a_g^2q^2\right),$$
$$h_N(q) = \sin\theta\,[h_{NR}(0) + ih_{NI}(0)]\exp\left(-\tfrac{1}{4}a_h^2q^2\right). \qquad (9)$$

Here $n = Ze^2/\hbar v = 0.0541$, v is the velocity of the incoming proton in the laboratory system, μ is the magnetic moment of the proton ($\mu = 2.79$ nuclear magnetons), $2n\ln(\theta_0/\theta)$ is the average difference between the Coulomb phase shifts in the region of the Coulomb and nuclear scatterings, $\theta_0 = 1.06/ka$; the imaginary part of $g_C(q)$ was assumed equal to 0 for $\theta \geq \theta_0$, when the phase shifts of the Coulomb scattering become of the same order as in nuclear scattering.

The differential elastic scattering cross section $d\sigma/d\omega(q)$ and the proton polarization $P(q)$ were determined by the expressions:

$$\frac{d\sigma}{d\omega}(q) = |g_N(q) + g_C(q)|^2 + |h_N(q) + h_C(q)|^2$$
$$= \frac{4n^2k^2}{q^4}\left(1 + \frac{m^2q^2}{k^2}\right)\exp\left(-\frac{a^2q^2}{2}\right)$$
$$+ [g_{NI}^2(0) + g_{NR}^2(0)]\exp\left(-\frac{a_g^2q^2}{2}\right)$$
$$+ \frac{q^2}{k^2}[h_{NI}^2(0) + h_{NR}^2(0)]\exp\left(-\frac{a_h^2q^2}{2}\right)$$
$$- \frac{4nk}{q^2}\left[g_{NR}(0) + 2n\ln\left(\frac{\theta_0}{\theta}\right)g_{NI}(0)\right]\exp\left[-\frac{(a_g^2 + a^2)q^2}{4}\right]$$
$$+ \frac{4nm}{k}\left[h_{NI}(0) - 2n\ln\left(\frac{\theta_0}{\theta}\right)h_{NR}(0)\right]\exp\left[-\frac{(a_h^2 + a^2)q^2}{4}\right], \qquad (10)$$

$$\frac{d\sigma}{d\omega}(q)P(q) = 2\,\mathrm{Re}\{[g_N(q) + g_C(q)]^*[h_N(q) + h_C(q)]\}$$
$$= 2\frac{q}{k}\left\{[g_{NR}(0)h_{NR}(0) + g_{NI}(0)h_{NI}(0)]\right.$$
$$\times \exp\left[-\frac{(a_g^2 + a_h^2)q^2}{4}\right]$$
$$+ \frac{2nmk}{q^2}\left[g_{NI}(0) - 2n\ln\left(\frac{\theta_0}{\theta}\right)g_{NR}(0)\right]\exp\left[-\frac{(a_g^2 + a^2)q^2}{4}\right]$$
$$\left. - \frac{2nk}{q^2}\left[h_{NR}(0) + 2n\ln\left(\frac{\theta_0}{\theta}\right)h_{NI}(0)\right]\exp\left[-\frac{(a_h^2 + a^2)q^2}{4}\right]\right\}, \qquad (11)$$

where $m = [\hbar^2k^2/2M^2c^2](\mu - 1/2)$. At 660 MeV we have $m = 1.918$.

B. Analysis of the experimental data. A search for the best set of independently varied parameters $g_{NR}(0)$, $g_{NI}(0)$, $h_{NR}(0)$, $h_{NI}(0)$, a_g, and a_h was made with the aid of the high-speed electronic computer of the Joint Institute for Nuclear Research. A standard computation program by the "gradient descent" method was employed [14] to find the minimum of the sum of the squares of the deviations

Values of nuclear amplitudes of pC scattering at 660 MeV (l. s.) and of the radial parameters of the Gaussian distribution, in units of 10^{-13} cm, together with the corresponding values of χ^2, γ_R, and γ_I, and also the calculated values of σ_t and σ_a.

Calculation variant	I	II	III	IV
Number of varied parameters N	4	5	5	6
Fixed parameters	$a_g = a_h = 1{,}965$	$a_g = a_h$	$g_{NI}(0) = 16{,}7 \pm 0{,}5$	
g_{NR} (0)	−5.81±0.31	−5.37±0.42	−3.61±0.15	−5,05±0.45
g_{NI} (0)	14.42±0.29	14.97±0.45		15.26±0.45
a_g		2.011±0.04	2.111±0.018	2.021±0.34
h_{NR} (0)	−29.5±6.8	−31.2±9.2	−6.7±13.7	−10.4±13.3
h_{NI} (0)	19.5±4.1	20.4±4.1	38.2±7.6	37.6±9.3
a_h		2.011±0.04	2,33±0.12	2,31±0.13
$\bar{\chi}^2 = \chi^2/(21 - N)$	1.6	1,4	1.8	1.2
γ_R	1.456±0.048	1.470±0.067	1.574±0.070	1,505±0.068
γ_I	0.900±0.051	0.792±0.062	0.497±0.021	0.744±0.068
σ_t, mb	276.3±5.6	286.9±8.6		292.4±8.6
σ_a, mb	201.5±4.0	212.1±5.8	242.7±0.6	217.2±5.8

$$\chi^2 = \sum_{i=1}^{2s} (\varepsilon_i/\Delta_i)^2,$$

where ϵ_i is the deviation of the calculated i-th value of the quantity under consideration from the corresponding experimental value, determined with an error Δ_i; the total set of the measurement results included twelve values of $d\sigma/d\omega(q)$ and nine values of P(q). It was assumed that the positive sign of the polarization corresponds to the direction of the polarization vector along the normal $\mathbf{n} = [\mathbf{k}_i \times \mathbf{k}_f]/|\mathbf{k}_i \times \mathbf{k}_f|$, where $\mathbf{k}_i$ and $\mathbf{k}_f$ are the wave vectors of the proton before and after scattering. From the obtained values of the varied parameters we calculated the values of the total cross section σ_t of the interaction between the protons and the carbon nuclei and the corresponding absorption cross section σ_a. The connection between $g_{NI}(0)$ and σ_t is given by the optical theorem

$$g_{NI}(0) = k\sigma_t/4\pi. \qquad (12)$$

The cross section σ_a is given by

$$\sigma_a = \pi a_g^2 [\ln(2\gamma_R) + C - \mathrm{Ei}(-2\gamma_R)], \qquad (13)$$

where a_g is the radial parameter of the form factor of the amplitude $g_N(q)$, and C = 0.577. The values of the real and imaginary parts γ_R and γ_I of the averaged phase $\gamma = \rho e^{i\varphi}$ of the nucleon-nucleus scattering was determined from the relations [see [14], formula (4.25)]

$$g_{NR}(0) = -\frac{1}{2} k a_g^2 \sum_{n=1}^{\infty} (-1)^{n-1} \frac{\rho^n \sin n\varphi}{n!n},$$

$$g_{NI}(0) = \frac{1}{2} k a_g^2 \sum_{n=1}^{\infty} (-1)^{n-1} \frac{\rho^n \cos n\varphi}{n!n}. \qquad (14)$$

The sums in (14) were tabulated with an electronic computer in steps of 0.05 for values $1 \le \rho \le 4$ and in steps of 1° for $0 \le \varphi \le 90°$. The values of ρ and φ were chosen to satisfy the obtained values of $g_{NR}(0)$ and $g_{NI}(0)$. According to the curves given by Greider and Glassgold [15], which represent the experimentally obtained values of σ_t and σ_a over a wide range of energies, we have at 660 MeV [2)]

$$\sigma_t(p + C) = (320 \pm 10) \cdot 10^{-27} \text{cm}^2,$$

$$\sigma_a(p + C) = (225 \pm 10) \cdot 10^{-27} \text{cm}^2.$$

It follows from (12) that the indicated value of σ_t corresponds to $g_{NI}(0) = (16.7 \pm 0.5) \times 10^{-13}$ cm.

Altogether, four variants were calculated. The results of the calculations are listed in the table. Figures 4 and 5 show the calculated angular dependences of the differential elastic-scattering cross sections and the proton polarization in this process.

Variant I. For all amplitudes of the nuclear scattering, the radial parameter was assumed to be the same and equal to $a = 1.965 \times 10^{-13}$ cm. This approximation is equivalent to neglecting the angular dependence of nucleon-nucleon scattering amplitudes. The value obtained for $g_{NI}(0)$ does not yield a sufficiently good value of σ_t. A similar

[2)] A somewhat different value of $\sigma_t(p + C)$ was obtained by Moskalev and Gavrilovskii [16].

situation obtains in the case of a four-parameter analysis of the data of pC scattering at 310 MeV, using $a = 1.965 \times 10^{-13}$ cm [4,12].

Variant II. The calculation was carried out under the assumption that the radial parameters a_g and a_h are equal to each other, but differ from $a = 1.965 \times 10^{-13}$ cm. Such a five-parameter approximation improves the agreement of the calculated cross sections σ_t and σ_a with experiment only slightly, and leads to a radial parameter 2.6% larger than the value obtained from electron scattering.

Variant III. The value $g_{NI}(0) = (16.7 \pm 0.5) \times 10^{-13}$ cm, obtained from the total cross section σ_t by the optical theorem, was fixed but the remaining five parameters were varied. It turns out here that $a_h > a_g > 1.963 \times 10^{-13}$ cm. The calculated cross section σ_a exceeds the measured one by about 10%.

Variant IV. A six-parameter search for the solution is made. An important factor here is that in this case $a_h > a_g > 1.965 \times 10^{-13}$ cm. The calculations yield the experimental value of σ_a, but the value obtained for σ_t is approximately 10% lower than the experimental ones.

C. Discussion of numerical results. The quality of the approximation, in accordance with the χ^2 criterion, is apparently best in the case of the six-parameter solution. If we assume the results of this solution to be correct, we can reach the conclusion that the mean-square radii corresponding to the amplitudes $g_N(0)$ and $h_N(q)$ are equal to, respectively,

$$\langle r_g^2 \rangle^{1/2} = \sqrt{3/2}\, a_g = (2.48 \pm 0.04) \cdot 10^{-13} \text{ cm},$$
$$\langle r_h^2 \rangle^{1/2} = \sqrt{3/2}\, a_h = (2.83 \pm 0.16) \cdot 10^{-13} \text{ cm},$$

and are noticeably larger than the mean-square radius obtained from the electron scattering. One must think that this difference is due to the finite radius of action of the nuclear forces, as a consequence of which the optical potentials of the nucleon-nucleus interaction extend somewhat farther than the distribution of nuclear matter.

The analysis performed offers undisputed evidence that at 660 MeV the real part of the spinless amplitude $g_{NR}(0)$ is negative and, consequently, the interference between the Coulomb and nuclear scatterings is constructive. This can be verified directly by considering the angular dependence of the quantity $[d\sigma/d\omega - d\sigma_C/d\omega]/F^2(q)$ where

$$\frac{d\sigma_C}{d\omega} = \left(\frac{Ze^2}{2\omega\beta^2}\right)^2 \frac{1}{\sin^4(\theta/2)} \frac{1}{[1 + kR\sin^2(\theta/2)]^2}$$

is the differential cross section for the scattering by an angle θ in the Coulomb field of a nucleus with uniformly distributed charge Ze and radius R [17]; w and βc are the total energy and velocity of the proton. It turns out that for $\theta > 2.5°$ this difference is practically independent of the angle while for $\theta < 2.5°$ it begins to increase with decreasing angle. Indications that the interference of the Coulomb and nuclear scatterings is more likely to be constructive were obtained earlier [10] from an analysis of the angular dependence of the differential pp-scattering cross section at 657 MeV. In this connection it should be noted that the quantity $g_{NR}(0)$ is positive and equal to 6.5×10^{-13} cm at 135 MeV [18] and 1.7×10^{-13} cm at 310 MeV [4] (see also [19], Table 9). Judging from the values of $g_{NR}(0)$ at 135, 310, and 660 MeV, the energy dependence $g_{NR}(0)$ can be represented in first approximation by a straight line, so that $g_{NR}(0)$ reverses sign at approximately 400 MeV. An analogous conclusion follows from an examination of the ratio of the real part of the central optical potential to its imaginary part as calculated by Batty [20]. This ratio is equal to zero near ~400 MeV. Only at this energy, strictly speaking, is it correct to consider the diffraction pattern of elastic scattering of nucleons by nuclei on the basis of the "black disc" model.

We did not bridge completely in the calculations a certain gap between the values of the imaginary part of the spinless amplitude $g_{NI}(0)$ obtained, on the one hand, from an analysis of the differential elastic-scattering cross section and the polarization, and on the other hand with the aid of the optical theorem. It is possible that the value of $g_{NR}(0)$ can be increased somewhat by further separate variation of the radial parameters of the form factors of the real and imaginary parts of the amplitudes $g_N(0)$ and $h_N(0)$.

The real part of the spin-dependent amplitude $h_{NR}(0)$ turns out to be very sensitive to changes in the radial parameter and is negative in all the variants of the calculations. The last two variants of the calculations indicate that the absolute value of $h_{NR}(0)$ is close to zero. One must think that if the analysis is extended to include the results of new more accurate small-angle measurements of the proton polarization and particularly measurements of the triple-scattering parameter A, it will be possible to obtain more reliable information on the value of the amplitude $h_{NR}(0)$. The imaginary part of the spin-dependent amplitude $h_{NI}(0)$ is clearly positive and has in the case of computation variants III and IV an absolute value appreciably larger than $h_{NR}(0)$.

4. CALCULATION OF pC-SCATTERING AMPLITUDES IN THE BORN APPROXIMATION AND OF THE OPTICAL-MODEL PARAMETERS AT 660 MeV

In the case of the scattering of a nucleon by a spinless nucleus, the potential of the optical model with account of the finite radius of interaction [12] can be written in the form

$$V(r) = V_C(r) + V_S(r)(\sigma \mathbf{L})$$
$$= 2\pi \frac{\hbar^2 c^2}{E}\left[-G(0)\,v(r) + \frac{H(0)}{k^2}\,u(r)\,(\sigma \mathbf{L})\right], \qquad (15)$$

where E is the total energy of the nucleon in the laboratory system; $V_C(r)$ and $V_S(r)$ are respectively the central and the spin-orbit potentials:

$$v(r) = [2\pi^2 G(0)]^{-1} \int_0^\infty G(q) F(q) J_0(qr)\, q^2 dq,$$

$$u(r) = -[2\pi^2 H(0)]^{-1} \int_0^\infty H(q) F(q) J_1(qr)\, q^3 dq; \qquad (16)$$

$J_0(qr)$ and $J_1(qr)$ are Bessel functions of zero and first order; G(q) and H(q) are the scattering amplitudes in the Born approximation:

$$f_{\text{Born}} = G(q) F(q) + H(q) F(q) \sin\theta \cdot \sigma_n. \qquad (17)$$

The values of the real and imaginary parts of the Born forward-scattering amplitudes G(0) and H(0) were calculated from data on the six-parameter solution from the following relations [see [4], formula (41.18) and [19], formula (6.8)]

$$\gamma = -2iG(0)/ka_g^2, \qquad (18)$$

$$H_R(0) = \left(1 + \tfrac{1}{4}\gamma_R\right) h_{NI}(0) + \tfrac{1}{4}\gamma_I h_{NR}(0), \qquad (19)$$

$$H_I(0) = -\left(1 + \tfrac{1}{4}\gamma_R\right) h_{NR}(0) + \tfrac{1}{4}\gamma_I h_{NI}(0). \qquad (20)$$

The following values were obtained as a result:

$$G(0) = ((-10{,}0 \pm 1{,}0) + i\,(20.2 \pm 1{,}1)) \cdot 10^{-13} \text{ cm},$$
$$H(0) = ((50 \pm 13) + i\,(21 \pm 18)) \cdot 10^{-13} \text{ cm}.$$

Knowing the amplitudes of the forward scattering in the Born approximation, we can calculate the integrated central and spin-orbit potentials U and W, respectively, per nucleon. An advantage of these potentials is that they depend little on the assumed form of the radial distribution of the nucleons and on the nuclear dimensions. These potentials are given by the expressions:

$$U = (2\pi\hbar^2 c^2 / EN)\, G(0), \qquad (21)$$

$$W = (2\pi\hbar^2 c^2 / ENk^2)\, H(0), \qquad (22)$$

where N is the number of nucleons in the nucleus.

The obtained values of the integrated potentials are:

$$U = ((-127 \pm 12) + i\,(257 \pm 14)) \cdot 10^{-39} \text{ MeV} \cdot \text{cm}^3,$$

$$W = ((14.8 \pm 3{,}9) + i\,(6.3 \pm 5\,4)) \cdot 10^{-65} \text{ MeV} \cdot \text{cm}^5.$$

This advantage is not possessed by the ordinary potentials of the optical model, the values of which can be estimated from the equations

$$V_C = NU / \Omega_g, \qquad V_S = NW / \Omega_h (\hbar/\mu c)^2,$$

where $\hbar/\mu c$ is the Compton wavelength of the pion; $\Omega_g = \pi^{3/2} a_g^3$ and $\Omega_h = \pi^{3/2} a_h^3$ are the volumes of the interaction region, corresponding to Gaussian distributions of the nuclear potentials. Using the obtained values of a_g, a_h, U, and W we obtain

$$V_{CR} \approx -33 \pm 3 \text{ MeV}, \qquad V_{CI} \approx 67 \pm 4 \text{ MeV},$$

$$V_{SR} \approx 1.3 \pm 0.3 \text{ MeV}, \qquad V_{SI} \approx 0.55 \pm 0.48 \text{ MeV}.$$

An indication of the presence of a real part in the central potential of the nucleon-nucleus interaction at 660 MeV was also obtained in [16,21].

It is important that at 660 MeV the spin-orbit potential is complex, with $W_i/W_R \approx 0.5$. The presence of an imaginary part in the spin-orbit potential offers evidence that in nucleon-nucleon collisions the formation of mesons in states with different values of j but identical values of l proceeds in different manners.

For 660-MeV protons the spin-orbit interaction parameter c, defined as the ratio.

$$c = |H(0)|/k^2 |G(0)|, \qquad (23)$$

is equal to $(0.056 \pm 0.015) \times 10^{-26}$ cm^2, which is practically one order of magnitude smaller than the values in the nuclear-shell model, and much smaller than the value obtained as a result of an analogous analysis of the data on the pC scattering at 310 MeV (see [4], Table 11). This means that the intensity of the spin-orbit interaction becomes definitely weaker over the extent of the considered energy interval.

In conclusion it must be emphasized that using a nucleon-nucleus scattering matrix written in a most general form we can, by excluding inelastic processes, tie in quantitatively all the available data on interactions between protons and carbon nuclei at 660 MeV. It is seen at the same time that $g_{NR}(0)$ is negative. The fact that the amplitude $g_{NR}(0)$ reverses sign over the energy interval from 310 to 660 MeV is evidence that the repelling action of the rigid "core" in nucleon-nucleon collisions becomes stronger with increasing energy.

The magnitude of the imaginary part of the spin-orbit potential has been determined with low accuracy, but it can nevertheless be stated that an analysis of the considered experimental data leads to a complex spin-orbit potential. The real part of this potential has the same sign as the spin-orbit potential in the shell model.

In principle, knowledge of the absolute values of the amplitudes of the nucleon-nucleus scattering within the framework of the superposition model of the nucleus, can by itself cast light on some elements of the nucleon-nucleon scattering matrix and help in the future with a phase-shift analysis of the pp and np scattering data in the considered energy region.

The authors are grateful to S. M. Bilen'kiĭ, R. M. Ryndin, and Ya. A. Smorodinskiĭ for useful discussions.

[1] H. Faissner, Ergebn. Exakten Naturwiss. **32**, 180 (1959).

[2] I. Levintov. DAN SSSR **107**, 240 (1956), Soviet Phys. Doklady **1**, 175 (1957).

[3] H. Köhler, Nucl. Phys. **1**, 433 (1956).

[4] H. Bethe, Ann. of Phys. **3**, 190 (1958).

[5] Brown, Ashmore, and Nordhagen. Proc. Phys. Soc. **71**, 565 (1958).

[6] L. Wolfenstein. Ann. Rev. Nucl. Sci. **6**, 43 (1956).

[7] Azhgireĭ, Kumekin, Meshcheryakov, Nurushev, Stoletov, and Huang. DAN SSSR, **145**, 1249 (1962), Soviet Phys. Doklady **7**, 737 (1963).

[8] V. Balashev and A. Tulinov, JETP **43**, 702 (1962), Soviet Phys. JETP **16**, 498 (1963).

[9] Azhgireĭ, Vzorov, Zrelov, Meshcheryakov, Neganov, Ryndin, and A. Shabudin, JETP **36**, 1631 (1959), Soviet Phys. JETP **9**, 1136 (1959).

[10] Meshcheryakov, Nurushev, and Stoletov, JETP, **33**, 37 (1957), Soviet Phys. JETP **6**, 28 (1958).

[11] Akimov, Savchenko, and Soroko, JETP **35**, 89 (1958), Soviet Phys. JETP **8**, 64 (1959).

[12] A. Cromer. Phys. Rev. **113**, 1607 (1959).

[13] Y. Fregeau, Phys. Rev. **104**, 225 (1956).

[14] S. Sokolov and I. Silin, Preprint Joint Inst. Nuc. Res., D-810 (1961).

[15] K. Greider and A. Glassgold. Ann. Phys. **10**, 100 (1960).

[16] V. Moskalev and B. Gavrilovskiĭ, DAN SSSR **110**, 972 (1956), Soviet Phys. Doklady **1**, 607 (1957).

[17] E. Williams. Proc. Roy. Soc. **A169**, 531 (1939).

[18] R. Wilson. Phys. Rev. **114**, 260 (1959).

[19] Kerman, McManus, and Thaler, Ann. of Phys. **8**, 551 (1959).

[20] C. Batty. Nucl. Phys. **23**, 562 (1961).

[21] Kozodaev, Kulyukin, Sulyaev, Filippov, and Shcherbakov, JETP **38**, 708 (1960), Soviet Phys. JETP **11**, 511 (1960).

Translated by J. G. Adashko
34